

# Recent Results from Jefferson Lab

Volker D. Burkert<sup>†</sup>

*Jefferson Lab, Newport News, Va. 23606, USA*

Recent results on studies of the structure of nucleons and nuclei in the regime of strong interaction QCD are discussed. Use of high current polarized electron beams, polarized targets, and recoil polarimeters, in conjunction with modern spectrometers and detector instrumentation allow much more detailed studies of nucleon and nuclear structure than has been possible in the past. The CEBAF accelerator at Jefferson Lab was build to study the internal structure of hadrons in a regime where confinement is important and strong interaction QCD is the relevant theory. I discuss how the first experiments already make significant contributions towards an improved understanding of hadronic structure.

## 1 Introduction

Electromagnetic production of hadrons may be characterized according to distance and time scales (or momentum and energy transfer) probed in the interaction. This is illustrated with the three regions in Figure 1. For simplicity I have omitted the time scale. At large distances mesons and nucleons are the relevant degrees of freedom. Due to the limited spatial resolution of the probe we study peripheral properties of nucleon and nuclei near threshold for pion production. Chiral perturbation theory describes many of these processes and has a direct link to QCD via (broken) chiral symmetry. At short distances (and short time scales), the coupling involves elementary quark and gluon fields, governed by perturbative QCD, and we map out parton distributions in the nucleon. At intermediate distances, quarks and gluons are relevant, however, confinement is important, and they appear as constituent quarks and glue. We study interactions between these constituents via their excitation spectra and wave functions. This is the region where the connection to the fundamentals of QCD remains poorly established, and where JLab experiments currently have their biggest impact. This is the region I will be focusing on in this lecture. These regions are not strictly separated from each other but overlap, and the hope is that due to this overlap hadron structures may eventually be described in a more unified approach based on fundamental theories. Because the electro-magnetic and electro-weak probes are well understood, they are best suited to provide the data for such an endeavor. I will discuss recent data on studies of the intrinsic nucleon structure, and results from light nuclear targets,  ${}^2H$  and  ${}^3He$ .

---

<sup>†</sup>e-mail: burkert@jlab.org

# Exclusive Hadron Production

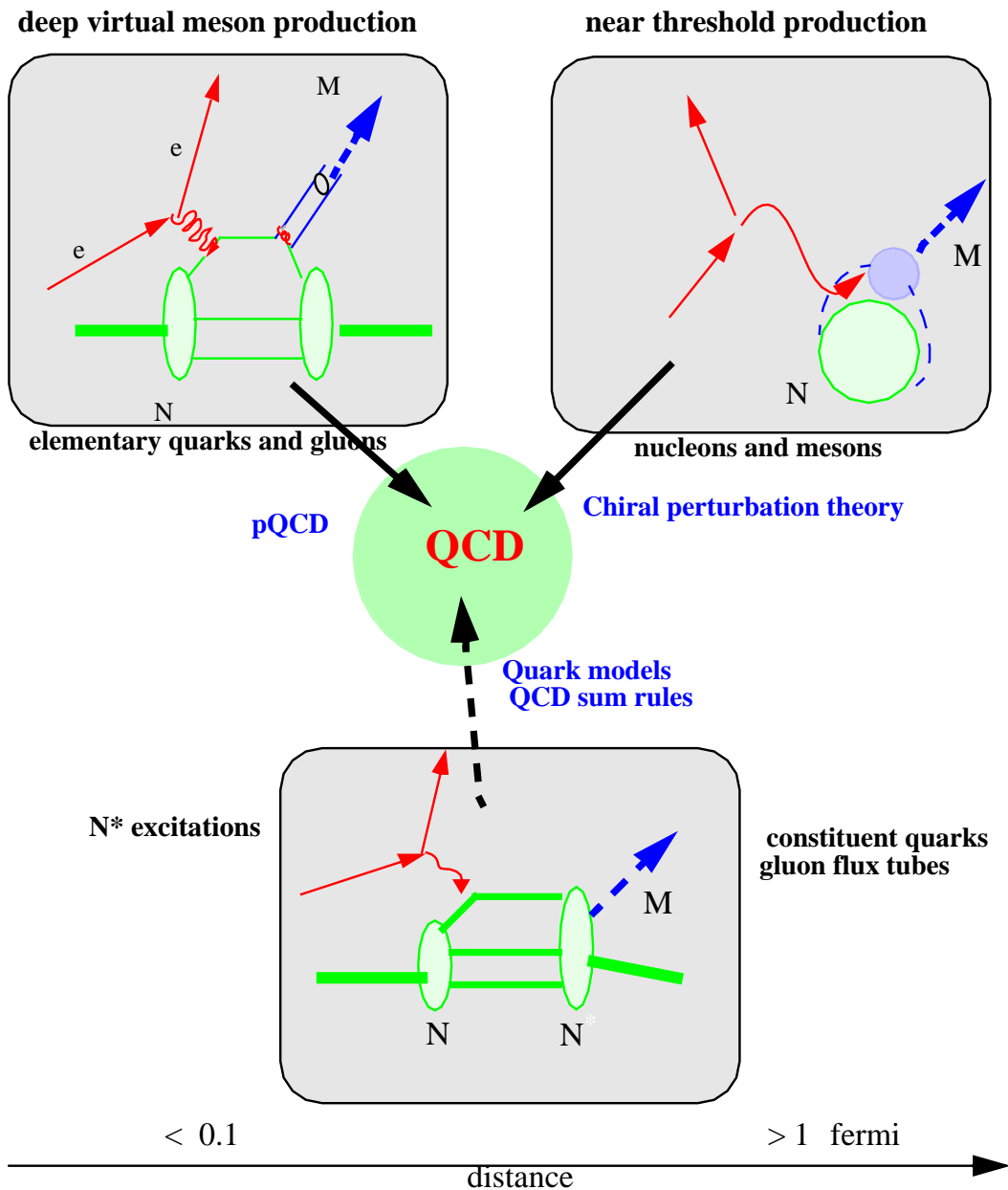


Fig. 1. Exclusive meson electroproduction. A subdivision in distance scales is used to illustrate three kinematic regions and their respective (effective) degrees of freedom.

## 1.1 Structure of the Nucleon at Intermediate Distances - Open Problems

QCD has not been solved for processes at intermediate distance scales. A direct consequence is that the internal structure of nucleons is generally poorly known in this regime. On the other hand, theorists are often not challenged due to the lack of high quality data in many areas. The following are areas where the lack of high quality data is most noticeable, and where JLab experiments have already contributed, or are expected to contribute significantly in the future:

- The electric form factors of the nucleon  $G_{En}$ ,  $G_{Ep}$  are poorly known, especially for the neutron, but also for the proton. This means that the charge distribution of the basic building blocks of the most common form of matter in the universe is virtually unknown.
- We do not know what role strange quarks play in the wave function of ordinary matter.
- The nucleon spin structure has been explored for more than two decades at high energies in laboratories such as CERN and SLAC. The confinement regime and the transition to the deep inelastic regime have not been explored at all.
- To understand the ground state nucleon we need to understand the full excitation spectrum as well as the continuum. Few transitions to excited states have been studied well, and many states are missing from the spectrum as predicted by our most accepted models.
- The role of the glue in the baryon excitation spectrum is completely unknown, although gluonic excitations of the nucleon are expected to be produced copiously [1].
- The long-known connection between the deep inelastic regime and the regime of confinement (local duality) [2] remained virtually unexplored for decades.

*Carrying out an experimental program that will address these questions has become feasible due to the availability of CW electron accelerators, modern detector instrumentation with high speed data transfer techniques, the routine availability of spin polarization in beam and targets and recoil polarimetry.*

The main contributor to this field is now the CEBAF accelerator at Jefferson Lab in Newport News, Virginia, USA. A maximum energy of 6 GeV is currently available. The three experimental halls (A, B, C) can receive polarized beam simultaneously, with different but correlated beam energies, or with the same beam energies. This allows a diverse physics program to be carried out in a very efficient way.

## 2 Structure of the Ground State Nucleon

### 2.1 Charge and current distribution

The nucleon ground state has been studied for decades in elastic electron-nucleon scattering. It probes the charge and current distribution in the nucleon in terms of the electric ( $G_E^\gamma$ ) and magnetic ( $G_M^\gamma$ ) form factors. The superscript  $\gamma$  or  $Z$  are used to describe the electromagnetic and weak form factor, respectively. Early experiments from Bonn, DESY, and CEA showed a violation of the so-called "scaling law", which may be interpreted that the spatial distribution of charge and magnetization are not the same, and the corresponding form factors have different  $Q^2$  dependencies. The data showed a downward trend for the ratio  $R_{EM}^\gamma = G_E^\gamma/G_M^\gamma$  as a function of  $Q^2$ . Adding the older and newer SLAC data sets confuses the picture greatly (Figure 2). Part of the data are incompatible with the other data sets. They also do not show the same general trend. Reliable data were urgently needed to clarify the experimental situation and to constrain theoretical developments.

Reliable data for the electric form factors at high  $Q^2$  can be obtained using double polarization measurements, and the first experiments of this type have now produced results. For a specific kinematics where the proton polarization is measured in the electron scattering plane, but transverse to the virtual photon, the double polarization asymmetry is given by:

$$A_{\bar{e}p} = \frac{k_1 R_{EM}^\gamma}{k_2 (R_{EM}^\gamma)^2 + k_3} ,$$

where the  $k_i$  are kinematic quantities. Since the ratio  $R_{EM}^\gamma$  is accessed directly this experiment has smaller systematic uncertainties than previous experiments at high  $Q^2$  (Figure 2). They confirm the trend of the early data, improve the accuracy at high  $Q^2$  significantly, and extend the  $Q^2$  range. The data illustrate beautifully the power of polarization in electromagnetic interactions. The experiment will be continued to higher momentum transfer in the year 2000. Other experiments[5, 6] will measure the same quantity on the neutron from a deuterium target using a similar techniques.

A precision measurement of neutron magnetic form factor will be carried out with CLAS using the neutron to proton ratio measured simultaneously [37]. This experiment will use the reaction  $ep \rightarrow en\pi^+$  for an in-situ calibration of the neutron counter detection efficiency.

### 2.2 Strangeness Structure of the Nucleon

From the analysis of deep inelastic polarized structure function experiments we know that the strange quark sea is polarized, and contributes at the 5 - 10% level to the nucleon spin. Then one may ask what are the strange quark contributions to the nucleon ground state wave function and their corresponding form factors? The flavor-neutral photon coupling does not distinguish s-quarks from u- or d-quarks. However, the tiny contribution of the  $Z^0$

is parity violating, and allows measurement of the strangeness contribution. The effect is measurable due to the interference with the single photon graph. The asymmetry

$$A_{\vec{e}p} = \frac{G_F Q^2}{\sqrt{2}\pi\alpha} \frac{\epsilon G_E^\gamma G_E^Z + \tau G_M^\gamma G_M^Z - \frac{1}{2}(1 - 4\sin^2\theta_W) K G_M^\gamma G_A^Z}{\epsilon(G_E^\gamma)^2 + \tau(G_M^\gamma)^2}$$

in polarized electron scattering contains combinations of electromagnetic and weak form factors. The term containing the axial form factor  $G_A^Z$  is suppressed due to the factor  $(1 - \sin^2\theta_W)$ , and gives small corrections. The weak form factors can be expressed in terms of the  $G^\gamma$  and the strangeness form factors ( $G^s$ ). For example, the weak electric form factor can be written:

$$G_E^Z = \left(\frac{1}{4} - \sin^2\theta_W\right) G_{Ep}^\gamma - \frac{1}{4}(G_{En}^\gamma + G_E^s)$$

The same relation holds for the magnetic form factors. The  $G^s$  form factors can be measured since the  $G^\gamma$  are known. The elastic  $\vec{e}p$  results of the JLAB HAPPEX experiment measured at  $Q^2 = 0.47 \text{ GeV}^2$ , show that strangeness contributions are small when measured in a combination of  $G_E^s$  and  $G_M^s$  [4]:

$$G_E^s + 0.4G_M^s = 0.023 \pm 0.034(\text{stat}) \pm 0.022(\text{syst}) \pm 0.026(G_E^n)$$

At least a factor of two smaller statistical error will be obtained when the 1999 data are included in the analysis. The error is then dominated by the uncertainties in the neutron electromagnetic form factor, especially  $G_{En}$ ! New measurements of  $G_{En}^\gamma$  and  $G_{Mn}^\gamma$  should remedy this situation [5, 6, 37].

### 3 The Nucleon Spin Structure - from Small to Large Distances

The internal spin structure of the nucleon has been of central interest ever since the EMC experiment found that at small distances the quarks carry only a fraction of the nucleon spin. Going from small to large distances the quarks get dressed with gluons and  $q\bar{q}$  pairs and acquire more and more of the nucleon spin. How is this process evolving with the distance scale? At the two extreme kinematic regions we have two fundamental sum rules: the Bjorken sum rule (Bj-SR) which holds in the asymptotic limit, and is usually written for the proton-neutron difference as

$$\Gamma_1^{pn} = \int g_1(x) dx = \frac{g_A}{6} .$$

At the finite  $Q^2$  where experiments are performed, QCD corrections have been calculated, and there is good agreement between theory and experiment at  $Q^2 > 2 \text{ GeV}^2$ . At the other end, at  $Q^2 = 0$ , the Gerasimov Drell-Hearn sum rule (GDH-SR) is expected to hold:

$$I_{GDH} = \frac{M^2}{8\pi^2\alpha} \int \frac{\sigma_{1/2}(\nu) - \sigma_{3/2}(\nu)}{\nu} d\nu = -\frac{1}{4}\kappa^2 .$$

The integral for the difference in helicity 1/2 and helicity 3/2 total absorption cross sections is taken over the entire inelastic energy regime. The quantity  $\kappa$  is the anomalous magnetic moment of the target.

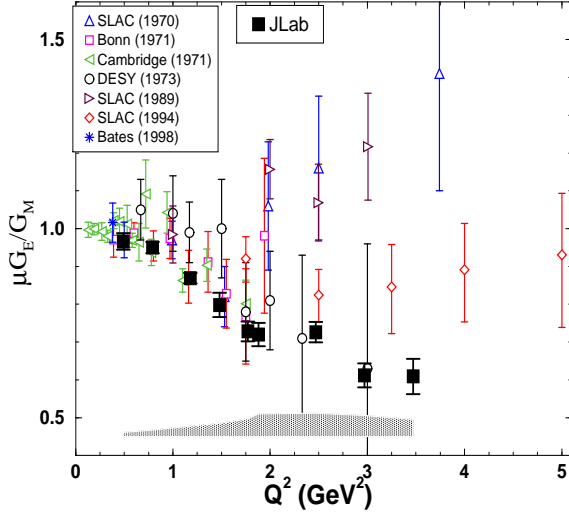


Fig. 2. Results for the ratio  $R_{EM}^\gamma$  of electric and magnetic form factors of the proton. The full squares are the results from JLAB obtained with the double polarization techniques [3]

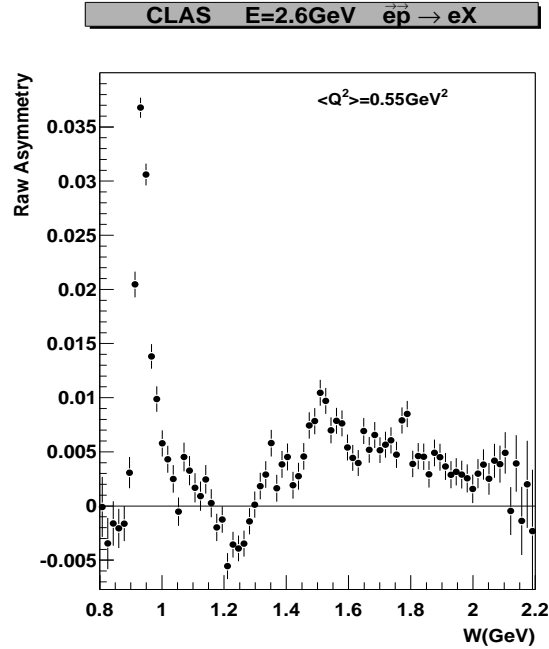


Fig. 3. Raw asymmetry measured in inclusive  $\vec{e}N\vec{H}_3 \rightarrow eX$  scattering at JLAB.

One important connection between these regions is given by the constraint due to the GDH-SR - it defines the slope of the Bjorken integral ( $\Gamma_1^{pn}(Q^2) = \int g_1^{pn}(x, Q^2) dx$ ) at  $Q^2 = 0$ :

$$I_{GDH}^{pn}(Q^2 \rightarrow 0) = 2 \frac{M^2}{Q^2} \Gamma_1^{pn}(Q^2 \rightarrow 0)$$

Phenomenological models have been proposed to extend the GDH integral for the proton and neutron to finite  $Q^2$  and connect it to the deep inelastic regime [8, 9, 7]. The data at low  $Q^2$  [10] are in good agreement with the predictions if nucleon resonances are taken into account explicitly [9] (Figure 4).

An interesting question is whether we can go beyond models and describe the transition from the Bj-SR to the GDH-SR for the proton-neutron difference within the framework of fundamental theory, i.e. QCD. For the proton and neutron, the GDH-SR is nearly saturated by low-lying resonances [11, 12] with the largest contributions coming from the excitation of the  $\Delta(1232)$ . The latter contribution is absent in the p-n difference. Other resonance contributions are reduced as well and the  $Q^2$  evolution may take on a smooth transition to the Bj-SR regime. A crucial question in this connection is: how low in  $Q^2$  the Bj-SR can be evolved using the modern techniques of higher order QCD expansion? Recent estimates

[13] suggest these techniques may be valid as low as  $Q^2 = 0.5 \text{ GeV}^2$ . At the other end, at  $Q^2 = 0$ , where hadrons are the relevant degrees of freedom, chiral perturbation theory may be applicable at very small  $Q^2$ , and may allow evolution of the GDH-SR to finite  $Q^2$ . Significant theoretical efforts are needed to bridge the remaining gap, perhaps utilizing lattice QCD. These efforts are of utmost importance since *it would mark the first time that hadronic structure is described by fundamental theory in the entire kinematic regime, from small to large distances!*

Experiments have been carried out at JLAB on  $NH_3$  [15],  $ND_3$ [16], and  $^3He$  [17] targets to extract the  $Q^2$  evolution of the GDH integral for protons and neutrons in the low  $Q^2$  range  $Q^2 = 0.1 - 2.0 \text{ GeV}^2$  and from the elastic to the deep inelastic regime. Currently, only two data points with large errors exist for  $Q^2 < 2 \text{ GeV}^2$ . Because of the current limitations in machine energy to 6 GeV, some extrapolation will be needed to determine the full integral, especially at the larger  $Q^2$  values. The deep inelastic contributions to the GDH integral have been measured for  $Q^2$  above  $1.3 \text{ GeV}^2$  [18]. First results from the JLAB experiments are expected in the year 2000. Figure 3 shows an uncorrected asymmetry from an experiment on polarized  $NH_3$ . The positive elastic asymmetry, the negative asymmetry in the  $\Delta$  region, and the changeover back to a positive asymmetry for higher mass resonances and the high energy continuum are evident.

## 4 Excitation of Baryon Resonances

A large effort is being extended to the study of excited states of the nucleon. The transition form factors contain information on the spin structure of the transition and the wave function of the excited state. We test predictions of baryon structure models and strong interaction QCD. Another aspect is the search for, so far, unobserved states which are missing from the spectrum but are predicted by the QCD inspired quark model [22]. Also, are there other than  $|Q^3 \rangle$  states? Gluonic excitations of the nucleon, i.e.  $|Q^3 G \rangle$  states may be copious /citeisgur, and some resonances may be “molecules” of baryons and mesons  $|Q^3 Q\bar{Q} \rangle$ . Search for at least some of these states is important to clarify the intrinsic quark-gluon structure of baryons and the role played by the glue and mesons in hadron spectroscopy and structure. Electroproduction is an important tool in these studies as it probes the internal structure of hadronic systems. The scope of the  $N^*$  program[24, 27] at JLAB is to measure many of the possible decay channels of resonances in a large kinematic range.

### 4.1 The $\gamma N \Delta$ transition.

The lowest excitation of the nucleon is the  $\Delta(1232)$  ground state. The electromagnetic excitation is due dominantly to a quark spin flip corresponding to a magnetic dipole transition. The interest today is in measuring the small electric and scalar quadrupole transitions which

## Ellis-Jaffe Integral

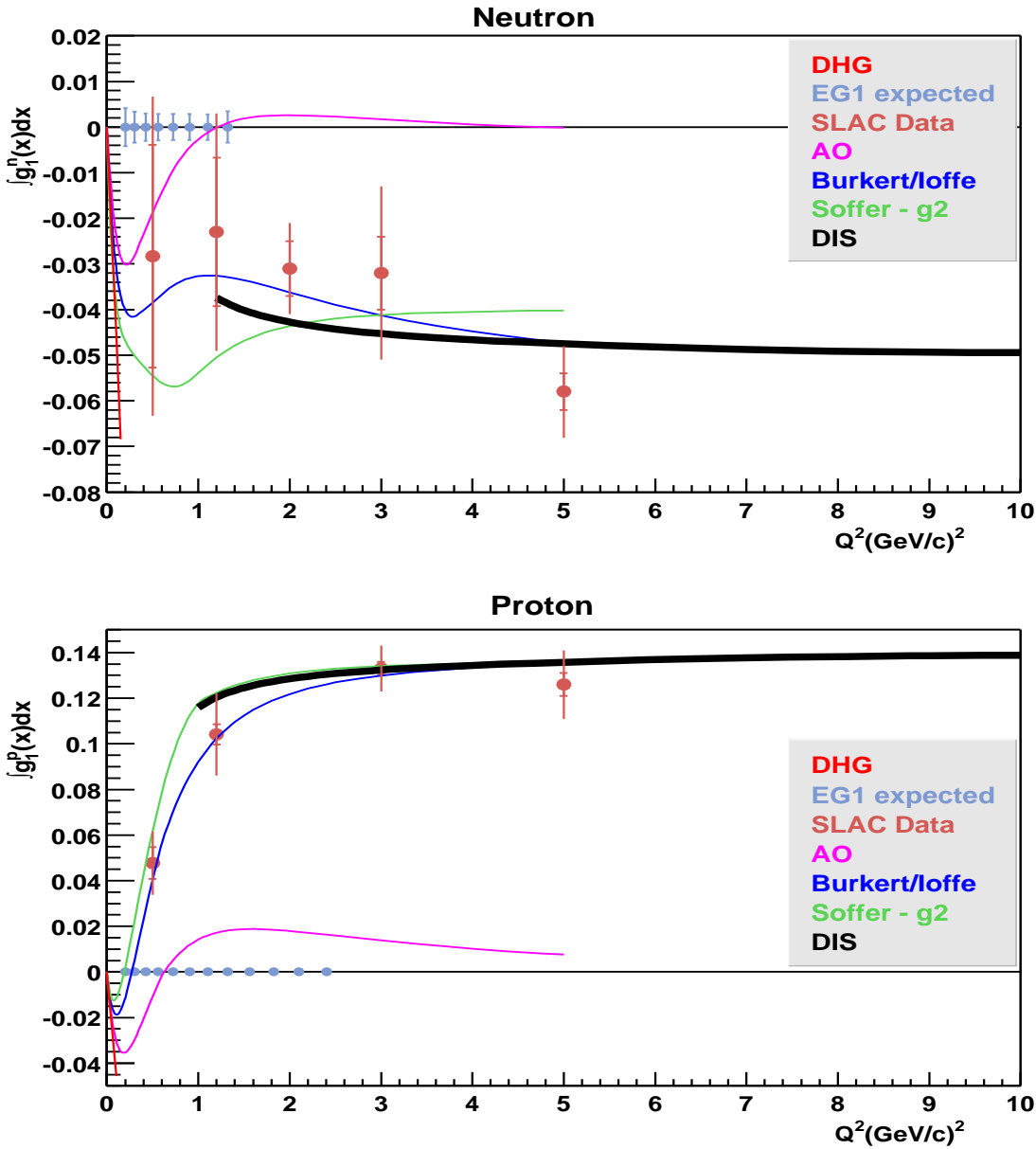


Fig. 4. The first moment  $\Gamma_1(Q^2)$  of the polarized structure function  $g_1(x, Q^2)$ . Model predictions from [7, 9]. The curve labelled AO contains s-channel resonance contributions only[11]. The straight line near  $Q^2 = 0$  is the slope given by the GDH sum rule constraint. The points along the horizontal axis indicate the expected statistical errors for the measured portion of the integral on the proton  $NH_3$  and neutron  $ND_3$ .



are predicted to be sensitive to possible deformation of the nucleon or the  $\Delta(1232)$  [23]. Contributions at the few percent level may come from the pion cloud at large distances, and gluon exchange at small distances. An intriguing prediction is that in the hard scattering limit the electric quadrupole contribution should be equal in strength to the magnetic dipole contribution [25]. An analysis [19] of earlier DESY data found small nonzero values for the ratio  $E_{1+}/M_{1+}$  at  $Q^2 = 3.2 \text{ GeV}^2$ , showing that the asymptotic QCD prediction is far away from the data.

An experiment at JLAB Hall C [20] measured  $p\pi^0$  production in the  $\Delta(1232)$  region at high momentum transfer, and found values for  $|E_{1+}/M_{1+}| < 5\%$  up to  $Q^2 = 4 \text{ GeV}^2$ . Analysis of new data from CLAS indicate negative values at small  $Q^2$  with a trend towards positive values at higher  $Q^2$ . Results should be available in 2000.

## 4.2 Higher mass resonances

The inclusive spectrum shows only 3 or 4 enhancements, however more than 20 states are known in the mass region up to 2 GeV. By measuring the electromagnetic transition of many of these states we can study symmetry properties between excited states and obtain a more complete picture of the nucleon structure. For example, in the single-quark-transition model only one quark participates in the interaction. It predicts transition amplitudes for a large number of states based on a few measured amplitudes [21]. The current situation is shown in Figure 5, where the SQTm amplitudes for the transition to the  $L_{3q} = 1 \text{ } SU(6) \otimes O(3)$  multiplet have been extracted from the measured amplitudes for  $S_{11}(1535)$ , and  $D_{13}(1520)$ . Predictions for other states belonging to the same multiplet are shown in the other panels. The lack of accurate data for most other resonances prevents a sensitive test of even the simple algebraic SQTm.

The goal of the  $N^*$  program at JLAB with the CLAS detector is to provide data in the entire resonance region, by measuring many channels in a large kinematic range, including many polarization observables. The yields of several channels recorded simultaneously are shown in Figure 6 and Figure 7. Resonance excitations seem to be. These yields illustrate how the various channels have different sensitivity to various resonance excitations. For example, the  $\Delta^{++}\pi^-$  channel clearly shows resonance excitation near 1720 MeV while single pion production is more sensitive to a resonance near 1680 MeV [27]. The  $p\omega$  channel shows resonance excitation near threshold, similar to the  $p\eta$  channel. No resonance has been observed in this channel so far. For the first time  $n\pi^+$  electroproduction has been measured throughout the resonance region, and in a large angle and  $Q^2$  range.

Figure 7 illustrates the vast improvement in data volume for the  $\Delta^{++}\pi^-$  channel. The top panel shows DESY data taken more than 20 years ago. The other two panels show samples of the data taken so far with CLAS. At higher  $Q^2$ , resonance structures, not seen before in this channel are revealed.

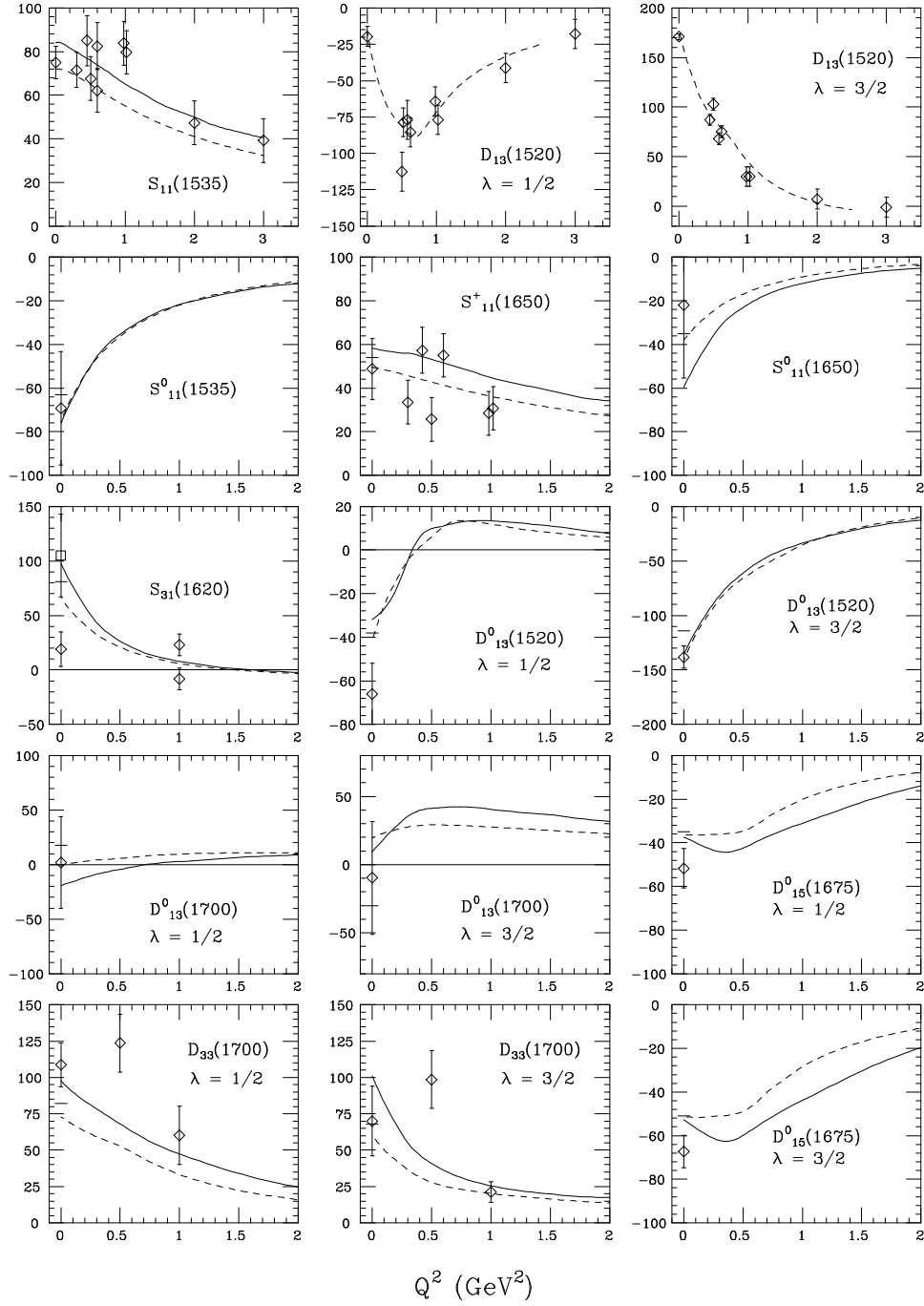


Fig. 5. Single Quark Transition Model predictions for states belonging to the  $SU(6) \otimes O(3)$  multiplet, discussed in the text.

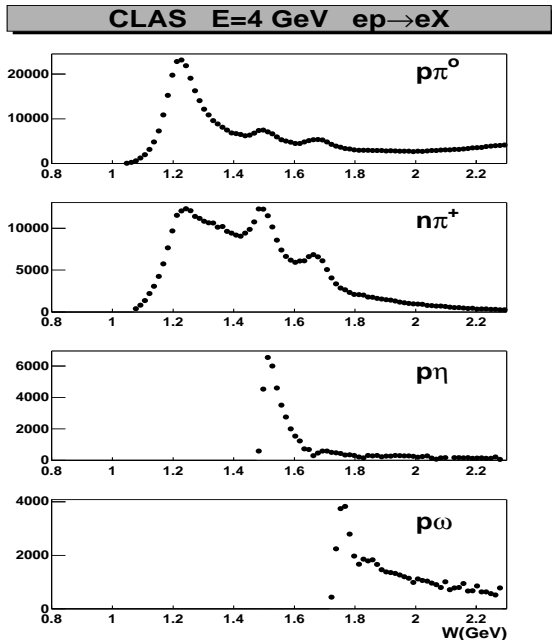


Fig. 6. Yields for various channels measured with CLAS at JLAB. The statistical error bars are smaller than the data points.

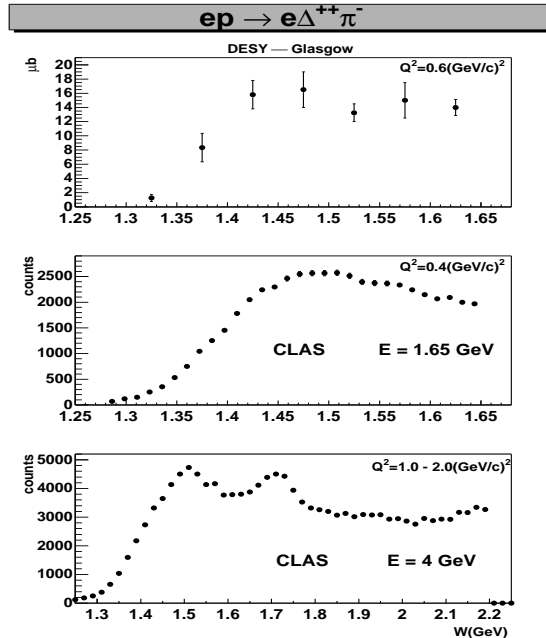


Fig. 7. Yields for the channel  $\Delta^{++}\pi^-$  measured with CLAS at different  $Q^2$  compared to previous data from DESY.

### 4.3 Missing quark model states

These are states predicted in the  $|Q^3\rangle$  model to populate the mass region around 2 GeV. However, they have not been seen in  $\pi N$  elastic scattering, our main source of information on the nucleon excitation spectrum.

How do we search for these states? Channels which are predicted to couple strongly to these states are  $N(\rho, \omega)$  or  $\Delta\pi$ . Some may also couple to  $KY$  or  $p\eta'$  [28].

Figure 8 shows preliminary data from CLAS in  $\omega$  production on protons. The process is expected to be dominated by diffraction-like  $\pi^0$  exchange with strong peaking at forward  $\omega$  angles, or low  $t$ , and a monotonic fall-off at large  $t$ . The data show clear deviations from the smooth fall-off for the  $W$  range near 1.9 GeV, where some of the “missing” resonances are predicted, in comparison with the high  $W$  region.

Although indications for resonance production are strong, analysis of more data and a full partial wave study are needed before definite conclusions may be drawn.

CLAS has collected  $5 \cdot 10^5$   $p\eta'$  events in photoproduction. Production of  $\eta'$  has also been observed in electron scattering for the first time with CLAS. This channel may provide a new tool in the search for missing states. The quark model predicts two resonances in this mass range with significant coupling to the  $N\eta'$  channel [28].

$K\Lambda$  or  $K\Sigma$  production may yet be another source of information on resonant states. Previous data show some evidence for resonance production in these channels [30]. New data

with much higher statistics are being accumulated with the CLAS detector, both in photo- and electroproduction. Strangeness production could open up yet another window for light quark baryon spectroscopy, which was not available in the past.

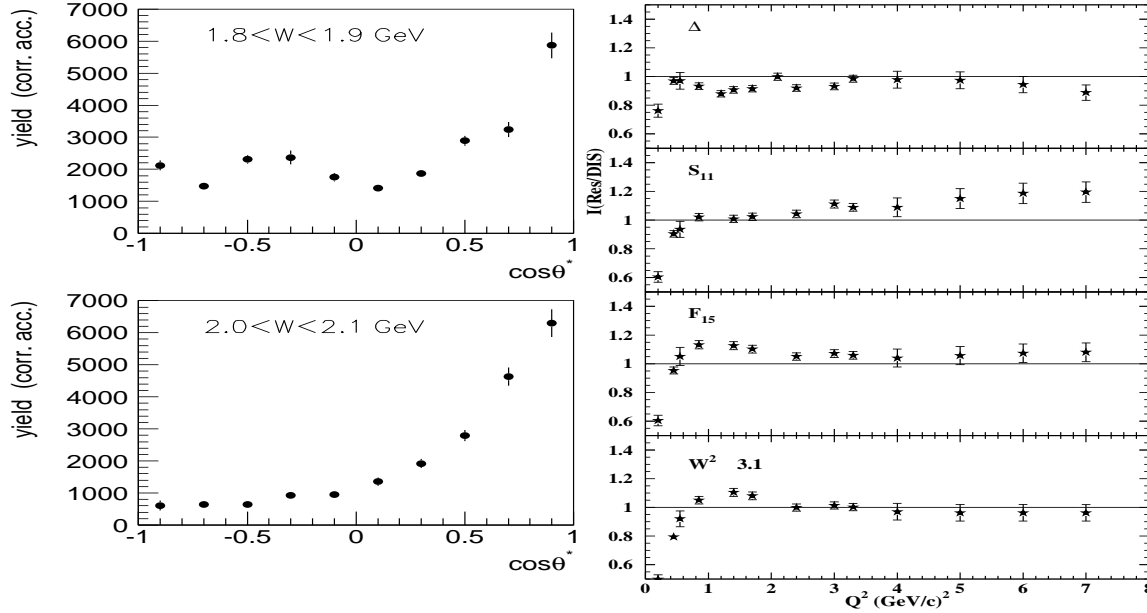


Fig. 8. Electroproduction of  $\omega$  mesons for different  $W$  bins. The deviation of the  $\cos\theta$ -distribution from a smooth fall-off for the low  $W$  bin suggests significant s-channel resonance production.

Fig. 9. Ratio of resonance excitations as observed and predicted from deep inelastic processes using quark-hadron duality.[29]

## 5 Local Duality - Connecting Constituent Quarks and Valence Quarks

I began my talk by expressing the expectation that we may eventually arrive at a unified description of hadronic structure from small to large distances. If such description is possible then there should be obvious connections in the data between these regimes. Such strong connections have indeed been observed by Bloom and Gilman [2]. They noted that the scaling curves from the deep inelastic cross section also describe the average inclusive cross sections in the resonance region if a scaling variable is chosen that takes into account target mass effects. Until recently, this intriguing observation was little utilized. A new inclusive ep scattering experiment at JLAB [29] helped rekindle the interest in this aspect of hadron physics. Remarkably, elastic form factors or resonance excitations of the nucleon can be predicted approximately from inclusive deep inelastic scattering data. Figure 9 shows the ratio of measured integrals over resonance regions, and predictions using deep inelastic data

only. The agreement is surprisingly good, though not perfect, indicating that the concept of duality likely is a non-trivial consequence of the underlying dynamics.

How can this success be explained in terms of the underlying degrees of freedom - elementary partons, and constituent quarks, respectively. Part of the answer is shown in Figure 10, where a large number of resonance data sets with different  $Q^2$  are shown together with the evolution curves from deep inelastic scattering. The deep inelastic curves fail to reproduce the resonance data at small  $\xi$ , while an evolution using valence quarks only has the same small  $\xi$  behavior. A new fit to the data (labelled JLab fit) reproduces the the  $xF_3(x)$  structure function determined from the difference of neutrino and anti-neutrino scattering (Figure 11) This quantity only contains valence quarks. The agreement suggests that the constituent quark distribution in the resonance region has an  $\xi$  dependence very similar to the distribution of elementary valence quarks in the deep inelastic region. It remains to be seen if this intriguing observation can be translated into the development of new model approaches to resonance physics.

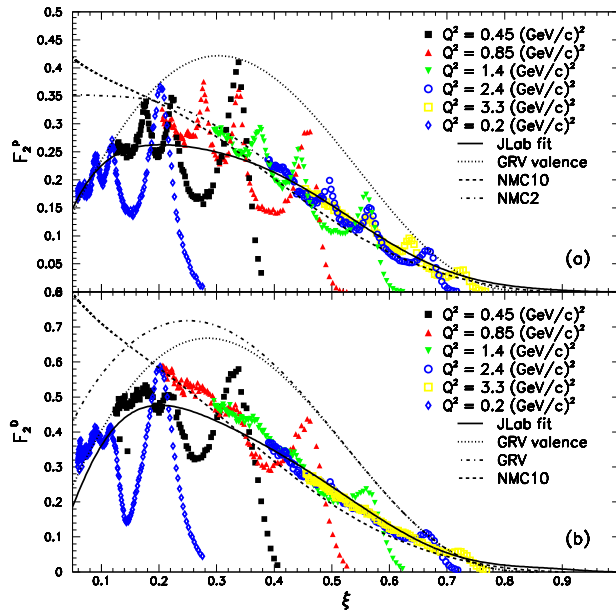


Fig. 10. Compilation of resonance data at different  $Q^2$ . The curves are from the evolution of deep inelastic data, with the exception of the curve labelled ‘JLab fit’ which represents a new fit to the JLab data.

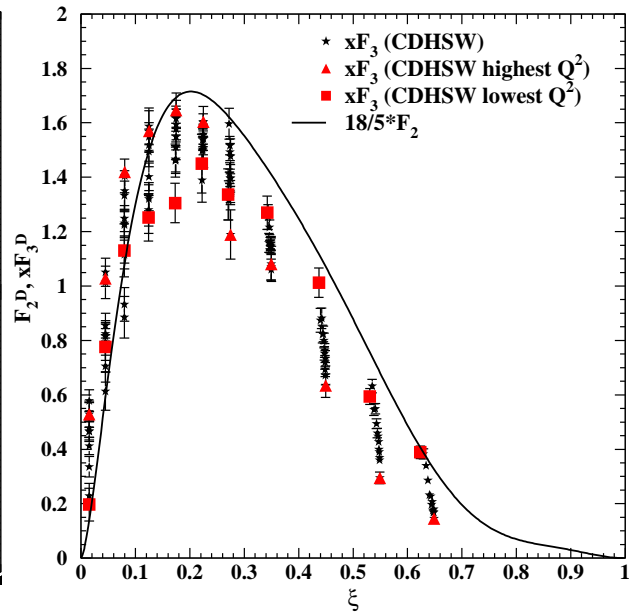


Fig. 11. The JLab fit to the  $F_2$  data from Figure 10 shown together with the  $xF_3$  structure function obtained from neutrino and anti-neutrino data. The latter represent the valence quark distribution in the nucleon.

In the following I will discuss recent results from experiments on  $^2H$  and  $^3He$ .

## 6 Elastic Formfactors of the Deuteron

In the same way that elastic electron scattering on protons and neutrons reveals their intrinsic charge and current distributions, so does elastic electron-deuteron scattering. Since the deuteron has spin 1, the elastic response functions contain 3 electromagnetic form factors  $G_C$ ,  $G_Q$ , and  $G_M$ . On the one hand, the interest in studying these form factors is to obtain a complete set of measurements. This involves measurement of at least one polarization observable ( $T_{20}$ ). On the other hand, there is significant interest in the high  $Q^2$  behavior. There we probe the short distance behavior of the nucleon-nucleon interaction. A large variety of models have been developed to describe the form factors for a wide range in distance scale, from hadronic models that include nucleons, pion, isobars, and exchange currents, descriptions within the quark exchange picture, to descriptions within the framework of perturbative QCD.

### 6.1 Unpolarized elastic response functions in $eD \rightarrow eD$

The unpolarized elastic eD scattering cross section contains the two response functions A, B:

$$\frac{d\sigma}{d\Omega} = \sigma_M [A(Q^2) + B(Q^2) \tan^2(\frac{\theta}{2})] \quad ,$$

where

$$A(Q^2) = G_C^2(Q^2) + \frac{8}{9}\tau^2 G_Q^2(Q^2) + \frac{2}{3}\tau G_M^2(Q^2)$$
$$B(Q^2) = \frac{4}{3}\tau(1 + \tau)G_M^2(Q^2); \quad \tau = \frac{Q^2}{4M^2}$$

Unpolarized electron scattering allows determination of the magnetic form factor by measuring the scattered electron at backward angles. A separation of  $G_C$  and  $G_Q$  is not possible. One can only separate the response functions  $A(Q^2)$  and  $B(Q^2)$  by measuring the elastic cross section at fixed  $Q^2$  and different scattering angles (Rosenbluth separation). An experiment in JLab Hall A (E-91-026) measured this process in a coincidence setup, where both the scattered electron and recoil deuteron were detected in two high resolution spectrometers. The results for  $A(Q^2)$  are shown in Figure 13.

The data are approximately described by modern hadronic models. Even the approach to scaling may therefore be understood within these models. It is therefore not obvious that quark-gluon degrees of freedom have to be invoked to describe the data even at the highest momentum transfers.

### 6.2 Tensor Polarization in $eD \rightarrow eD$

A separation of the charge and quadrupole form factors of the deuteron requires a polarization experiment, in addition to the unpolarized measurement. A measurement of the tensor

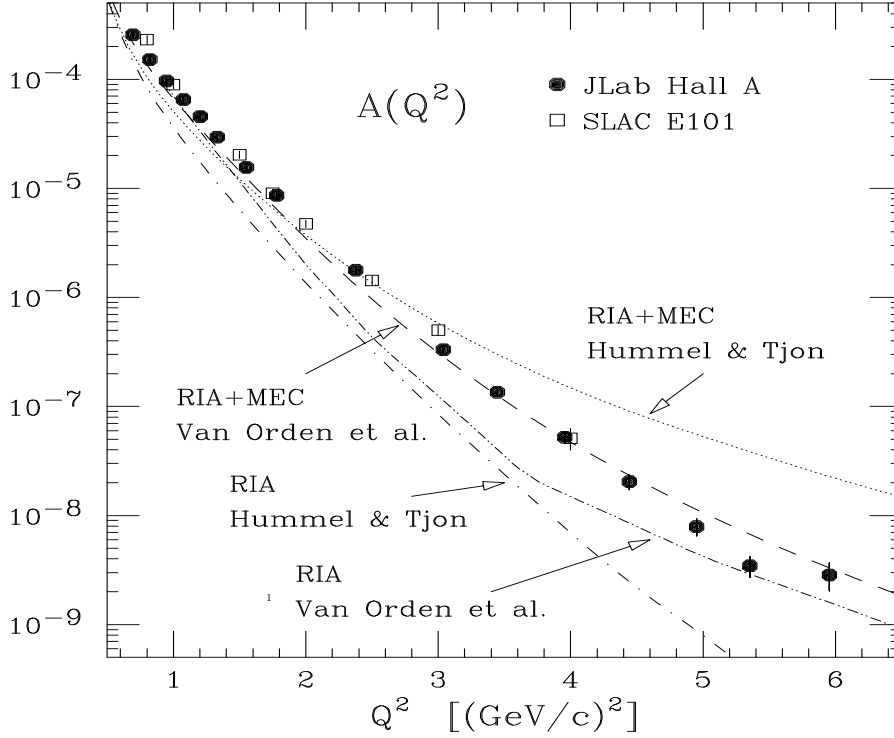


Fig. 12. The electric response function  $A(Q^2)$  measured in  $eD \rightarrow eD$  scattering. The JLab data extend the  $Q^2$  range from previous SLAC data.

polarization  $t_{20}$  is particularly suited to accomplish this. This tensor polarization component can be expressed in terms of the electromagnetic form factors:

$$t_{20} = -2 \frac{\tau G_Q (\tau G_Q + 3G_C)}{G_C^2 + \frac{8}{9} \tau^2 G_Q^2}$$

These experiments require a measurement of the deuteron recoil polarization in a second scattering experiment using a suitable analyzing reaction. Previous experiments of this type have been carried out at lower energy accelerators, covering the lower  $Q^2$  range. The JLab experiment was carried out in Hall C, using a high power deuterium cryogenic target, and a new deuteron magnetic spectrometer to analyze the kinematics and deuteron polarization. A liquid hydrogen target was used for the second scattering experiment, which was needed to analyse the deuteron polarization[31]. The results for  $t_{20}$  are shown in Figure 14 [32, 33]. Using the known response function  $A(Q^2)$  the deuteron charge form factor  $G_C(Q^2)$  can be separated (Figure 15). The charge form factor shows a zero crossing at  $Q^2 = 0.7 \text{ GeV}^2$ , and remains negative over the complete large  $Q^2$  range.

Hadronic models describe the data over the entire range in momentum transfer.

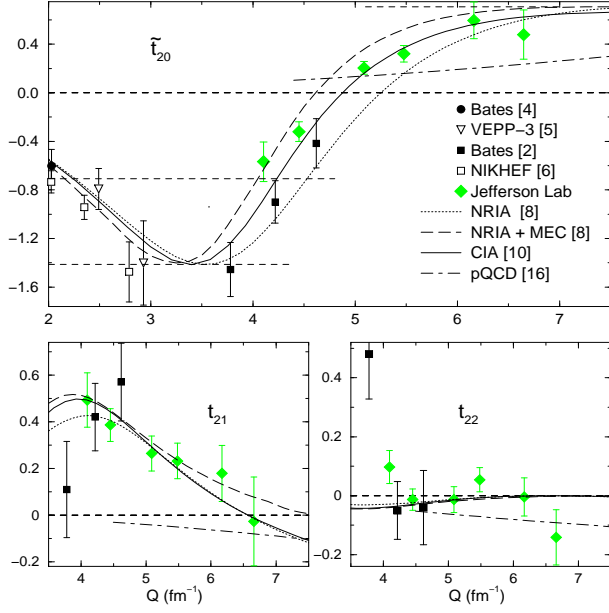


Fig. 13. The tensor polarizations  $t_{20}$ ,  $t_{21}$  and  $t_{22}$  measured in  $eD \rightarrow eD$ . The deuteron polarization was measured in  $Dp \rightarrow ppn$  scattering.

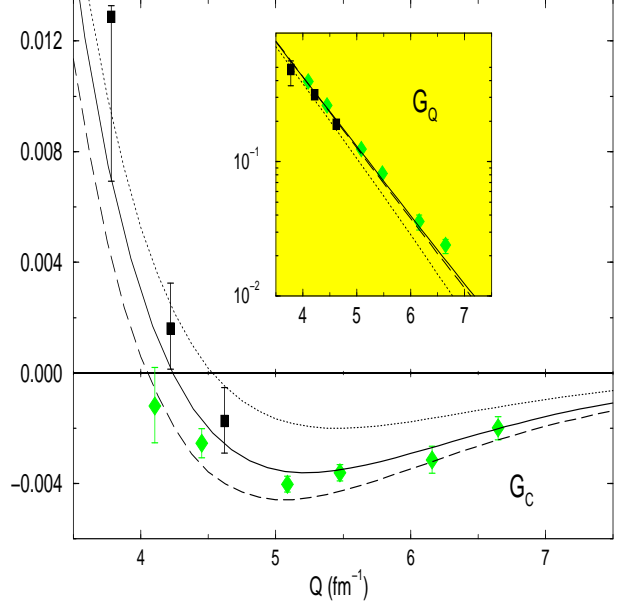


Fig. 14. The deuteron charge and quadrupole form factors as extracted from the  $t_{20}$  measurement and the known  $A(Q^2)$  response function.

### 6.3 Deuteron photo-disintegration at high momentum transfer

The deuteron is an ideal laboratory to study where the traditional Yukawan picture of the nucleus may break down, and the quark picture may provide a more effective description. The deuteron as the simplest nucleus permits exact hadronic calculations. Experimentally, one can give a large momentum transfer to the constituents, and thus study the approach to scaling at modest energies.

One of the indications for the relevance of quark constituents in the interaction is scaling of the differential cross section according to the number of constituents involved in the interaction. Constituent counting rules predict that the energy dependence for the two-body reaction  $\gamma d \rightarrow np$  should scale like:

$$\frac{d\sigma}{dt} = \frac{h(\theta_{cm})}{s^{n-2}},$$

where  $n$  is the number of elementary fields in the initial and final states, and  $n-2 = 11$  for the  $\gamma d \rightarrow np$ . While scaling has been observed at center-of-mass angles near  $90^\circ$  for photon energies as low as 1 GeV and up to the maximum energies of 4 GeV (Figure 16), no scaling is observed for smaller  $\theta_{cm}$  angles [34].

New models have been developed that give a more realistic description of the process, and predict the parameter  $n$  to be angle-dependent, e.g. the Regge gluon-string model [35], and quark exchange models where the number of constituent involved in the reaction is



smaller than in the maximal model ("constituent scaling") which involves all constituents. These models indeed provide a better description of the reaction over a larger kinematical range (Figure 17).

New data have been taken to extend the kinematic range up to 5.5 GeV photon energies to see whether scaling persists for the 90° kinematics, and if scaling is approached at different angles.

## 6.4 Polarization asymmetries on ${}^3\text{He}$

${}^3\text{He}$  has emerged as an attractive target material for polarized neutrons. It is the closest any nucleus comes to a pure polarized neutron target and is a simple enough nucleus, so that corrections to this naive picture can be calculated with some confidence. At low momentum transfer, corrections appear to be large for some reactions.

An experiment in JLAB Hall A measured quasi-elastic electron scattering off  ${}^3\text{He}$  in an effort to get information on the magnetic form factor of the neutron, and to study asymmetries in the breakup region at small excitation energies [36].

Figure 18 shows preliminary data for the sensitivity of the measured asymmetry to the neutron magnetic form factor. The model dependency of final state corrections seems small enough to allow extraction of the quantity of interest.

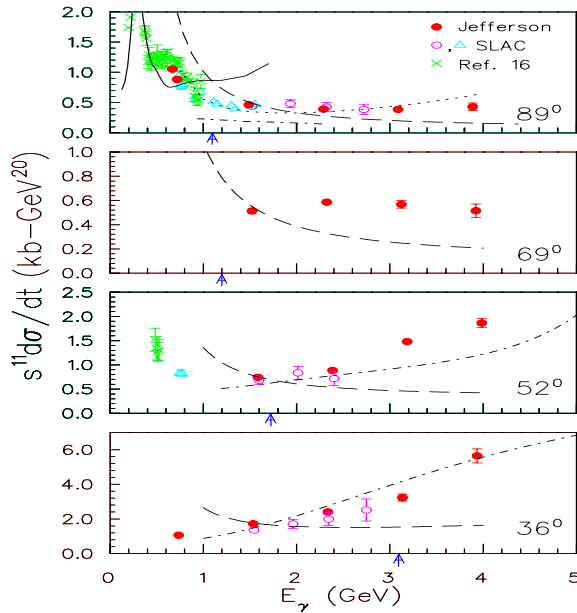


Fig. 15. The cross section for  $\gamma d \rightarrow np$  multiplied by the predicted dimensional scaling function  $s^{11}$ . Scaling is not observed at small angles, where the quark exchange model gives a better representation of the data.

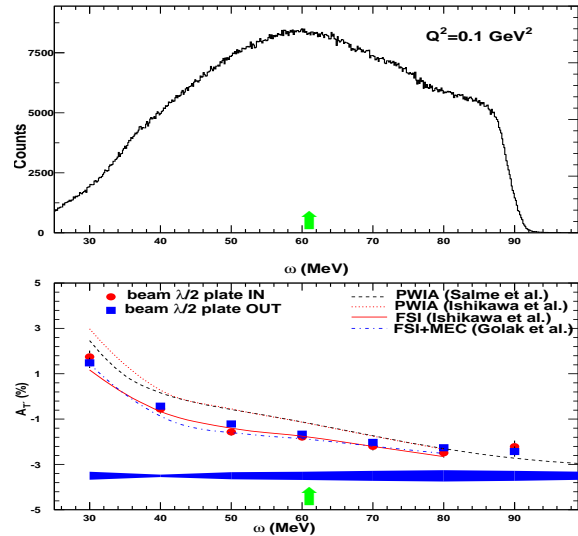


Fig. 16. Preliminary results for JLAB experiment E95-001 to measure the magnetic form factor of the neutron. The experimental asymmetry is shown measured in scattering of polarized electrons from a polarized  ${}^3\text{He}$  target.

## 7 Outlook

The ongoing experimental effort at Jefferson Lab will provide the community with a wealth of data in the first decade of the next millennium to address many open problems in hadronic structure at intermediate distances. *The experimental effort must be accompanied by a significant theoretical effort to translate this into real progress in our understanding of the complex regime of strong interaction physics.* One area, where a fundamental description may be within reach, is the evolution of the nucleon spin structure from small to large distances.

New instrumentation will become available, e.g. the  $G^o$  experiment at JLAB, allowing a broad program in parity violation to study strangeness form factors in electron scattering in a large kinematic range.

Moreover, there are new opportunities on the horizon. Recently, it was shown[38, 39] that in exclusive processes the soft (nonperturbative) part and the hard (perturbative) parts factorize for longitudinal photons at sufficiently high  $Q^2$ . A new set of “skewed parton distributions” can then be measured which are generalizations of the inclusive structure functions measured in deep inelastic scattering. For example, low- $t$   $\rho$  production probes the unpolarized parton distributions, while pion production probes the polarized structure functions. Experiments to study these new parton distributions need to have sufficient energy transfer and momentum transfer to reach the pQCD regime, high luminosity to measure the small exclusive cross sections, and good resolution to isolate exclusive reactions.

This new area of research may become a new frontier of electromagnetic physics well into the next century.

To accommodate new physics requirements, an energy upgrade in the 10-12 GeV range has been proposed for the CEBAF machine at JLAB. This upgrade will be accompanied by the construction of a new experimental hall for tagged photon experiments with a  $4\pi$  solenoid detector to study exotic meson spectroscopy, and production of other heavy mesons. Existing spectrometers in Hall C will be upgraded to reach higher momenta and improvements of CLAS will allow it to cope with higher multiplicities.

This will give us access to kinematics where copious hybrid meson production is expected, higher momentum transfer can be reached for form factor measurements, and we may begin to map out the new generalized parton distributions.

## References

- [1] N. Isgur, hep-ph/9904494, (1999)
- [2] E.D. Bloom and F.J. Gilman, Phys. Rev. D4, 2901 (1970)
- [3] M.K. Jones, et al., nucl-ex/9910005; see also: C. Perdrisat, plenary talk, Proceedings of PANIC99, June '99, Uppsala, Sweden

- [4] K.A. Aniol, et al., Phys. Rev. Lett. 82, 1096(1999)
- [5] D. Day, et al., JLAB experiment E93-026
- [6] R. Madey et al, JLAB experiment E93-038
- [7] J. Soffer and O. Teryaev, Phys.Rev.Lett. 70, 3373(1993)
- [8] V. Burkert and B. Ioffe, Phys.Letts. B296 (1992)223
- [9] V. Burkert and B. Ioffe, J.Exp.Theo.Phys. 78, 619 (1994)
- [10] K. Abe et al., Phys. Rev. D58, 2003 (1998)
- [11] V. Burkert and Zh. Li, Phys. Rev. D47, 46(1993)
- [12] W.X. Ma, D.H. Lu, A.W. Thomas, Z.P. Li, Nucl. Phys. A635 (1998) 497
- [13] X. Ji, J. Osborne, hep-ph/9905010 (1999)
- [14] X. Ji, C.W. Kao, and J. Osborne, hep-ph/9910256
- [15] V. Burkert, D. Crabb, R. Minehart et al., JLAB experiment E-91-023
- [16] S. Kuhn, M. Taiuti et al., JLAB experiment E93-009
- [17] Z. Meziani, et al., JLAB experiment E94-010
- [18] K. Ackerstaff et al., Phys. Letts. B444(1998)531
- [19] V. Burkert, L. Elouadrhiri, Phys. Rev. Lett. 75, 3614 (1995)
- [20] V. Frolov et al., Phys. Rev. Lett. 82, 45 (1999)
- [21] A.J. Hey , J. Weyers, Phys. Letts. 48B, 69 (1974)
- [22] N. Isgur, G. Karl, Phys. Rev. D23, 817 (1981)
- [23] V. Frolov et al., Phys. Rev. Lett. 82, 45 (1999)
- [24] V.D. Burkert, Nucl. Phys. A623 (1997) 59c-70c
- [25] C.E. Carlson, Phys. Rev. D34, 2704 (1986)
- [26] H. Funsten et al., JLab experiment E91-024; J. Manak et al., proceedings of PANIC99, June '99, Uppsala, Sweden
- [27] M. Ripani et al., Proceedings, PANIC99, June '99, Uppsala, Sweden

- [28] S. Capstick and W. Roberts, Phys. Rev. D49, 4570 (1994)
- [29] I. Niculescu et al., "Experimental Verification of Quark-Hadron Duality", R. Ent, C. Keppel, private communication
- [30] M. Q. Tran et al., Phys. Lett. B445, 20 (1998)
- [31] E. Beise, S. Kox et al., Jlab experiment E94-018
- [32] presented by: J.-S. Real, INFN Workshop on the Structure of the Nucleon, Trieste, Italy, May 1999.)
- [33] presented by K. Hafidi, PANIC 99 Uppsala, Sweden, June 1999.)
- [34] C. Bochna et al., Phys. Rev. Lett.81, 4576 (1998)
- [35] L. Kondratyuk, E. DeSanctis, et al., Phys. Rev. C (1993)
- [36] H. Gao et al., JLAB experiment E95-001
- [37] W. Brooks, et al., JLAB experiment E94-017
- [38] X. Ji, Phys. Rev. D55, 7114 (1997)
- [39] A. Radyushkin, Phys. Rev. D56, 5524 (1997)